Reprinted from *Current Science*

Tilings, coverings, clusters and quasicrystals

E. A. Lord*,#, S. Ranganathan* and U. D. Kulkarni†

*Department of Metallurgy, Indian Institute of Science, Bangalore 560 012, India
†Materials Science Division, Bhabha Atomic Research Centre, Trombay, Mumbai 400 085, India

A quasiperiodic covering of the plane by regular decagons and an analogous structure in three dimensions are described. The 3D pattern consists of interpenetrating triacontahedral clusters, related to the τ^3 inflation rule for the 3D Penrose tiling patterns. The overlap regions are triacontahedron faces, rhombic dodecahedra and rhombic icosahedra. The structure leads to a plausible model for the T2 icosahedral quasicrystalline phases.

SINCE the first discovery of a quasicrystalline phase[1] the number of different varieties of quasicrystals has become quite large. The elucidation of the detailed atomic structure of these alloys has called forth new concepts and methods. The traditional methods of crystallography are inadequate; even such basic concepts as lattices and unit cells are inapplicable. Two theoretical approaches, separately and in conjunction, have proved valuable. In the 'tiling patterns' approach the tiles of a quasiperiodic tiling pattern (usually the two rhombuses of the Penrose patterns[2,3] or the two rhombic hexahedra[4,5] that are their three-dimensional analogues) are decorated by 'atoms' – in a manner similar to the description of a periodic structure in terms of the decoration of a unit cell. The discovery that quasiperiodic tiling patterns with rhombic or rhombohedral tiles can arise from a projection of a (periodic) lattice in a higher-dimensional[6] space has given rise to a large body of literature. Another approach is based on the concept of clusters of atoms joined together by sharing of atoms to build an aperiodic structure – clusters possessing icosahedral symmetry giving rise to structures with long-range orientational order with icosahedral or decagonal symmetry.

Icosahedral atomic clusters

In both the 'tiling' approach and the 'cluster' approach, model building is guided by knowledge of known structures of the crystalline (i.e. periodic) phases that are closely related to quasicrystalline phases. These 'approximants' occur together with the quasi-crystalline phases and share grain boundaries with them, hence they clearly have microstructures similar to those of quasicrystals. An early example, in which the tiling approach and the cluster approach were successfully combined is the 3D quasiperiodic structure deduced from the periodic α(AlMnSi) phase[7] – a bcc structure in which the 54-atom Mackay icosahedron occurs as a structural unit. An alternative model consists of aluminium icosahedra with octahedral linkages along their three-fold axes[8].

The structures of decagonal AlMn phases consist essentially of towers of icosahedra with their axes along the periodic direction, packed in a quasiperiodic arrangement. Contiguous towers are related by a two-fold rotation about an axis perpendicular to the periodic axis. Li[9] has deduced the quasiperiodic structure of the (flat and puckered) layers perpendicular to the periodic axis in terms of decorations of a tiling pattern involving three tile shapes[10].

The 'clustering' picture is obviously closer to the reality of the way quasicrystals actually grow (though one should not discount the value of the concept of decorated tilings – after all, the 'unit cells' of a periodic crystal have no bearing on the way atoms actually combine to build the structure!). A cluster is conceived to grow by accretion; successive shells of atoms are added to an initial seed such as a 12- or 13-atom icosahedron. The clusters bond to each other by sharing of atoms. They can be quite large. Of particular importance are the 54-atom Mackay icosahedron[11] and the 44-atom Bergman unit or Pauling triacontahedron[12]. A cluster of 102 atoms with icosahedral symmetry occurs as a building block in $Mg_{32}(Al, Zn)_{49}$ (refs 12 and 13). In the remarkable R-AlCuLi bcc structure[13,14] the bcc positions are centres of 136-atom clusters which overlap (in the sense of having shared atoms) to produce a large cubic unit cell of 154 atoms. An even larger cluster containing 14 shells and a total of 498 atoms can be identified[13,15]. The vacant bcc positions lie at their centres and eight of the vertices of the fourteenth shell (a lithium dodecahedron). The R phase is closely related to the quasicrystalline T2 phase[16]. Romeau and Aragon[17] claim that the seventh shell has cubic symmetry in the R phase (24 atoms at the vertices of the Archimedean polyhedron (3.4^3), i.e. the semi-regular figure with an equilateral triangle and three square faces surrounding each vertex) whereas in the quasicrystalline T2 phase it has 6 extra atoms and forms an icosidodecahedron (3.5.3.5).

Romeau and Aragon[17] have investigated the way in which overlapping clusters can build quasiperiodic struc-

#For correspondence (e-mail: lord@metalrg.iisc.ernet.in)

tures. Starting from an icosahedral seed or a 19-atom seed in the form of a pair of icosahedra sharing a double pentagonal pyramid, special 'O-points' arise at some stage of the accretion that can act as centres of a new cluster.

Janot[18] has drawn attention to the way in which clusters, 'bonded' by sharing atoms, appear to behave rather like atoms – at a larger scale. He has shown how electronic and other properties of quasicrystalline materials can be understood in terms of large clusters mimicking the behaviour of individual atoms.

Coverings of the plane

The first 'aperiodic' set of 2D tiles (i.e. a finite number of shapes that can tile the plane, but which cannot be arranged to form a periodic tiling pattern) consisted of over 20,000 tile shapes[19]! Penrose's discovery of an aperiodic set of only six tiles[2] and finally a set of only *two*[20] was an amazing event. Whether any aperiodic 'set' consisting of only one tile is possible is an open question. It seems unlikely. If one considers *coverings* of the plane rather than *tilings*, the situation is different. Gummelt[21] has produced a regular decagon decorated by black and white regions (Figure 1), copies of which can be superimposed, obeying the matching rule 'black on black, white on white', producing a quasiperiodic covering of the plane.

Gummelt's result can be most simply established by considering the Penrose 'kite and dart' patterns[22]. The patch shown in Figure 2, consisting of two kites and a dart, is called an 'ace' in Conway's terminology. The matching rules for assembling a kite and dart pattern (enforced by requiring the vertices to be 'black' or 'white' according to the scheme shown in Figure 1) imply Conway's theorem that, in a tiling of the plane by kites and darts satisfying the matching rule, *every point of the plane is part of an ace*. (This is very easily proved by considering the ways in which the white vertex at the reentrant angle of the dart, or the white vertex at the join of the two short edges can be surrounded.) There are just four ways (ignoring orientation) that a pair of aces can be joined to produce a larger patch. These are shown in Figure 3. Now decorate the kites and darts with black and white regions according to the scheme shown in Figure 4 and consider the black and white patterns that arise in the neighbourhood of an ace when further aces are added to it in the ways shown in Figure 3. We deduce that every ace (and hence, by Conway's theorem, every point of the pattern) lies in a decagonal region like Figure 1. Conver-

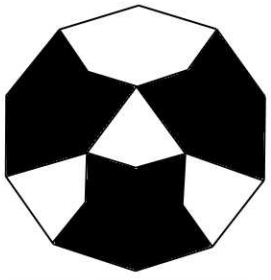

Figure 1. Gummelt's decagon.

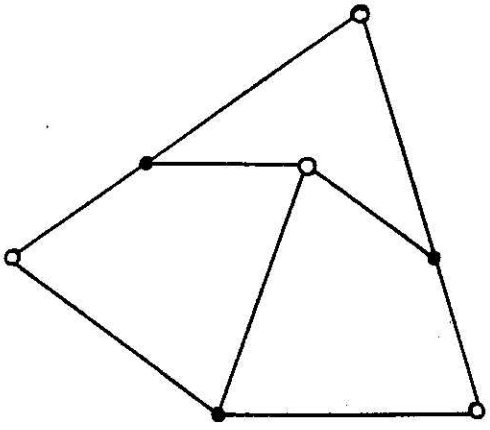

Figure 2. An 'ace' of a Penrose kite and dart pattern. The matching rule for the assembling of quasiperiodic kite and dart patterns is provided by colouring the vertices of the kites and darts, as indicated.

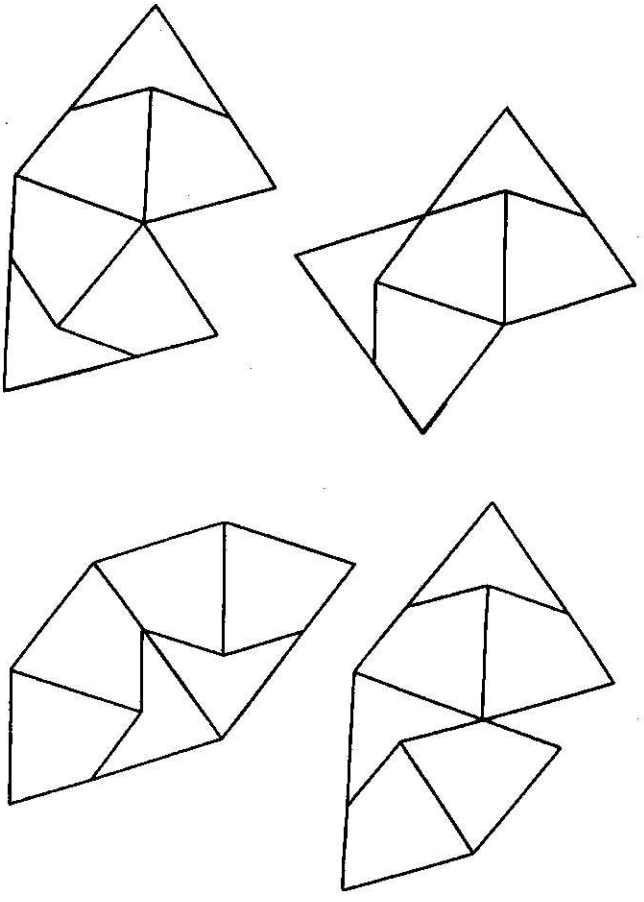

Figure 3. The four ways in which two aces can be combined.

sely, there are just four ways in which pairs of these decagons can overlap, black on black, white on white. Inscribing the associated aces in them, we recover Figure 3. This establishes that the decagon coverings and the kite and dart tilings are 'equivalent' (in the sense that the one can be converted to the other without ambiguity), and Gummelt's result is proved.

The 'cartwheel' employed in Gummelt's rather complicated proof can be obtained by applying two inflations[3] to an ace (Figure 5).

A model for the decagonal quasicrystalline phases of AlNiCo and AlCuCo, based on the concept of identically decorated overlapping decagons has been proposed by Burkov[23]. Jeong and Steinhardt[24] emphasized the important role that Gummelt's covering of the plane by identical decagons could play in the development of structural models of decagonal quasicrystalline phases, based on the clustering concept rather than the tiling concept. Very recently a successful model for the quasicrystalline phase of AlNiCo has been obtained in this way[25].

A *different* quasiperiodic covering of the plane by decagons can be seen simply by looking at a Penrose rhomb pattern; it is immediately obvious that these patterns contain overlapping regular decagons whose edges are edges of the tiles. These decagonal patches are of *two* kinds (Figure 6). Sasisekharan[26] has studied the Penrose patterns in terms of the covering of the plane by these decagons. The matching rules for the Penrose rhombs imply that, in the coverings of the plane by these decagons two contiguous decagons either abut along an edge, or overlap by sharing a thin rhomb, or overlap by sharing a hexagon (consisting of a fat rhomb and two thin rhombs). If the rhombic tiles that decorate the decagons are eliminated and the decagons decorated, instead, by three concentric rings of 'atoms', in the ratio $1 : \tau : \tau^2$ (where τ is the 'golden number' $(1 + \sqrt{5})/2$) we arrive at a 2D quasiperiodic structure comprising clusters *all of the same kind*. A pair of contiguous clusters can combine in just three different ways (Figure 7).

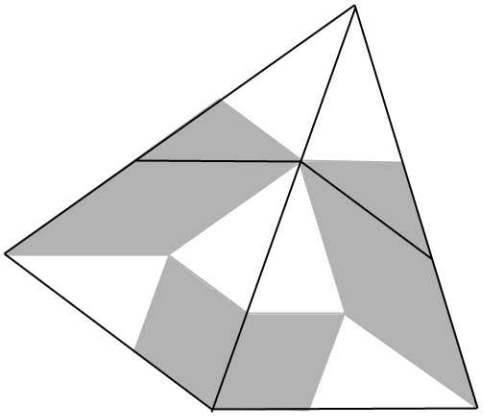

Figure 4. The decoration of the kites and darts that leads to Gummelt's patterns.

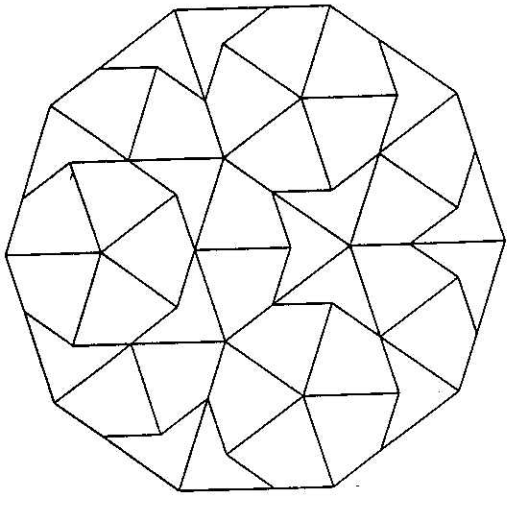

Figure 5. A 'cartwheel' in a kite and dart pattern.

Triacontahedral clusters

The coverings of the plane by the overlapping decagons in Penrose rhomb patterns have an analogue in three dimensions. The quasiperiodic space filling by hexahedral units contains overlapping triacontahedra (each consisting of 10 oblate + 10 prolate units). This was recognized by Mackay[27] who emphasized the importance of clusters with icosahedral symmetry in quasicrystal structure.

We shall now demonstrate the existence of a 3D analogue of the patterns produced by the decorated decagons of Figure 7. The analogue of the decagon in 2D patterns is a rhombic triacontahedron. The decagonal clusters of points have 10 external and 21 internal vertices. This pattern of 31 points arises by projection along the [11111] axis of the vertices of a 5D hypercube (the two hypercube vertices on the axis project to the single point at the centre

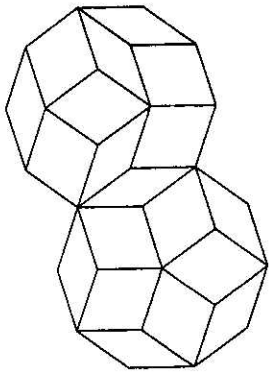

Figure 6. Two kinds of decagonal patch in a Penrose rhomb pattern.

of the decagon). In the construction of a decagon from 5 fat rhombs and 5 thin rhombs (Figure 6), only 6 of the 21 internal vertices appear. A 3D analogue of the decagonal cluster is obtained by projecting a 6D hypercube. The 64 vertices of the hypercube project to the 32 vertices of a *rhombic triacontahedron*, and 32 *internal vertices* (Figure 8).

Six orthogonal vectors of length $\gamma\sqrt{2}$ ($\gamma = \sqrt{(2+\tau)}$) in E_6 can be projected on to a 3D subspace, so that their images are the six vectors $\mathbf{e}_1, \ldots, \mathbf{e}_6$ given by the columns of

$$\begin{pmatrix} \tau & 0 & -1 & 0 & \tau & 1 \\ 0 & 1 & \tau & 1 & 0 & \tau \\ 1 & \tau & 0 & -\tau & -1 & 0 \end{pmatrix}.$$

The projected image a 6D hypercube of edge length $\gamma\sqrt{2}$ is then a rhombic triacontahedron of edge length γ. The 32 vertices of the triacontahedron, and the 32 internal vertices, are indicated in Figure 8. Position vectors in 3D are indicated by the following labelling system: $\mathbf{e}_1, \mathbf{e}_2, \ldots, \mathbf{e}_6$ are denoted by 1, 2, . . ., 6 and $\mathbf{e}_1 + \mathbf{e}_4 + \mathbf{e}_6$, for example, is denoted by 146. Figure 8 illustrates views along $\mathbf{e}_6$.

The 32 internal vertices are vertices of a pentagonal dodecahedron with an icosahedron inside it. Both have edge length $2/\tau$. The stellation of the small pentagonal dodecahedron gives the 12 five-fold external vertices; stellating the small icosahedron gives the 20 three-fold vertices (Figure 9).

The standard 3D generalization of the Penrose rhomb tiling patterns, consisting of the vertices of a spacefilling by two rhombic hexahedra, a *prolate unit* (PU) and an *oblate unit* (OU), arises as the projection of a slice of a 6D hypercubic lattice.

According to Mackay[28], it was Robert Amman who first recognized that the two units PU and OU are 3D analogues of the rhombic Penrose tiles. Accordingly, we shall refer to the standard 3D patterns as 'Amman patterns'.

They have a τ^3 inflation rule. The relationship between the Amman pattern of edge length τ^3 and the one of unit edge length associated with it is described by Audier and Guyot[13].

Every vertex of the τ^3 pattern is the centre of a *star polyhedron* comprising twenty prolate units (Figure 10). the mid-point of every edge of the τ^3 pattern is the centre of a *rhombic icosahedron* (Figure 11) (comprising 5 PU and 5 OU). These fit, in an obvious way, into the 'dimples' of the star polyhedra. The space in the interior of the τ^3

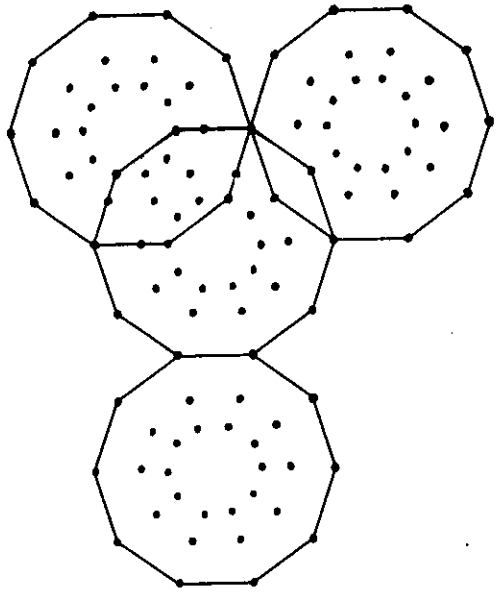

Figure 7. Three ways of combining the decagonal clusters: sharing an edge, a thin rhomb, or a hexagon.

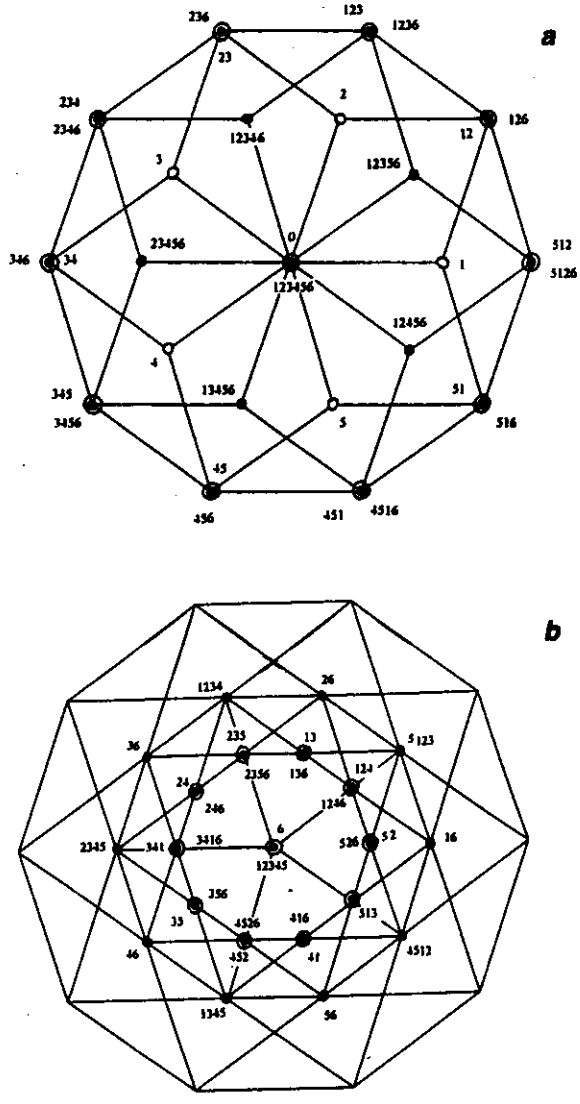

Figure 8. Projection of a 6D hypercube: *a*, the 32 external vertices; *b*, the 32 internal vertices.

PU is exactly filled by a pair of *rhombic triacontahedra* sharing a single OU at the mid-point of the three-fold axis of the τ^3 PU (Figure 12).

The two star polyhedra centred at the two vertices on the three-fold axis of a τ^3 OU overlap; they share one PU.

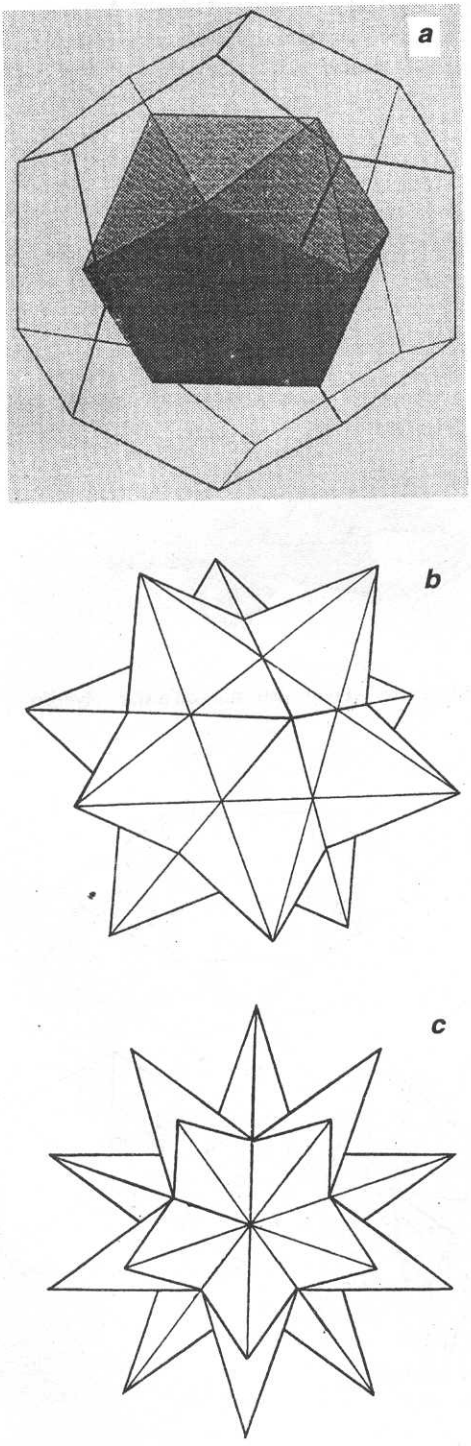

Figure 9. *a*, The 'small' icosahedron and the 'small' dodecahedron inside the 30-hedron; *b*, Stellation of the small dodecahedron; *c*, stellation of the small icosahedron.

The remaining spaces in the interior of the τ^3 OU are filled by a ring of six OUs surrounding this PU (Figure 13).

This completes the spacefilling by the hexahedron of unit edge length. Any Amman pattern must fit the description we have given. There remains scope for variations, of course, because a rhombic icosahedron can be built from 5 PU + 5 OU in more than one way, and the building of a rhombic triacontahedron from 10 PU + 10 OU is also not unique.

Figure 14 shows a ring of five OUs placed on a star polyhedron. When a *rhombic icosahedron* (RI) is placed in the resulting 'cup', we get a rhombic triacontahedron consisting of RI, five of the PUs of the star polyhedron and the five OUs that have been added. The centre of the star polyhedron is a vertex of the triacontahedron.

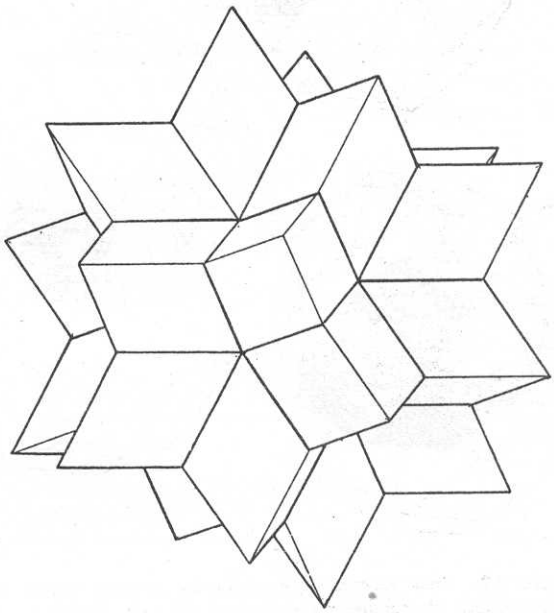

Figure 10. Star polyhedron consisting of 20 prolate hexahedra.

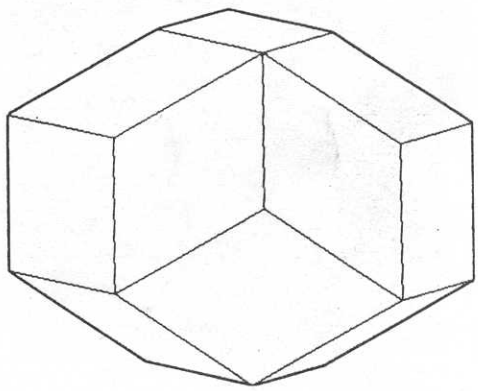

Figure 11. The rhombic icosahedron.

The mid-points of all the edges of the τ^3 pattern are centres of rhombic RI connecting a pair of stars. If we imagine all these icosahedra to be supplemented by ten OUs (five round the 'top' and five round the 'bottom'), we shall obtain a pattern in which every edge of the τ^3 pattern contains the centres of two triacontahedra. These triacontahedra overlap, the overlap region being the RI. The centres of the two triacontahedra are at golden mean positions on the τ^3 edge.

We now have arrived at description of a pattern of overlapping triacontahedra. (It should be noticed that it is *not* a complete covering of the space – the PU along the axis of every τ^3 OU is *not* contained in any of the triacontahedra.) Taking the triacontahedra to have unit edge length, their centres are related to a τ^3 Amman pattern in a simple way: *two centres lie on every τ^3 edge, at golden mean positions, and two centres lie at the golden mean positions on the long diagonal of every τ^3 PU.*

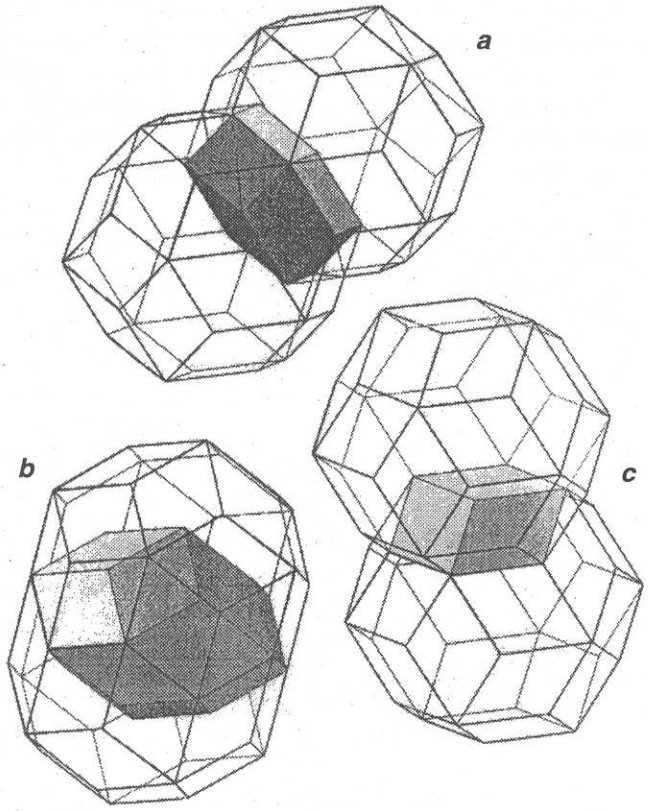

Figure 12. Two rhombic triacontahedra sharing (*a*) a rhombic dodecahedron; (*b*) a rhombic icosahedron; (*c*) a single oblate unit.

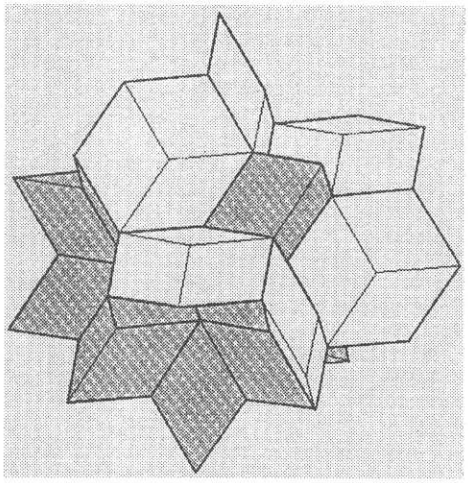

Figure 13. Six oblate units on a star polyhedron.

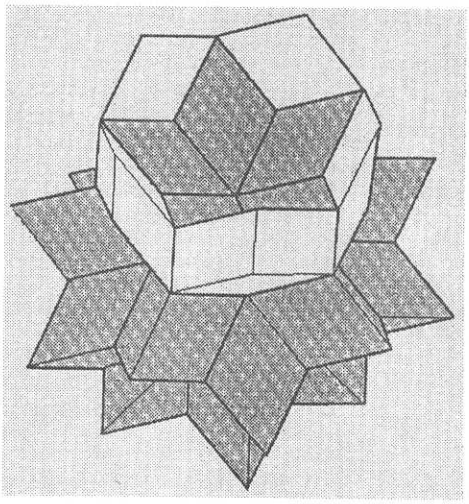

Figure 14. Five oblate units on a star polyhedron.

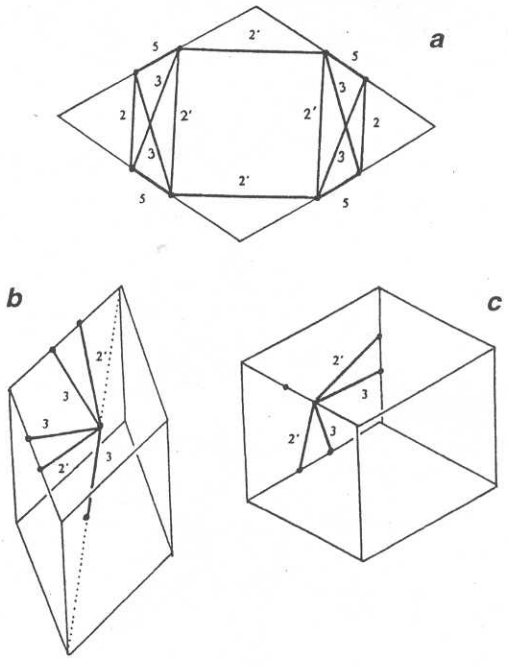

Figure 15. Lines of centres for overlapping pairs of 30-hedra, occurring in the τ^3 units. *a*, A face of a τ^3 unit (edge length is $\gamma\tau^3$); *b*, τ^3 PU; *c*, τ^3 OU.

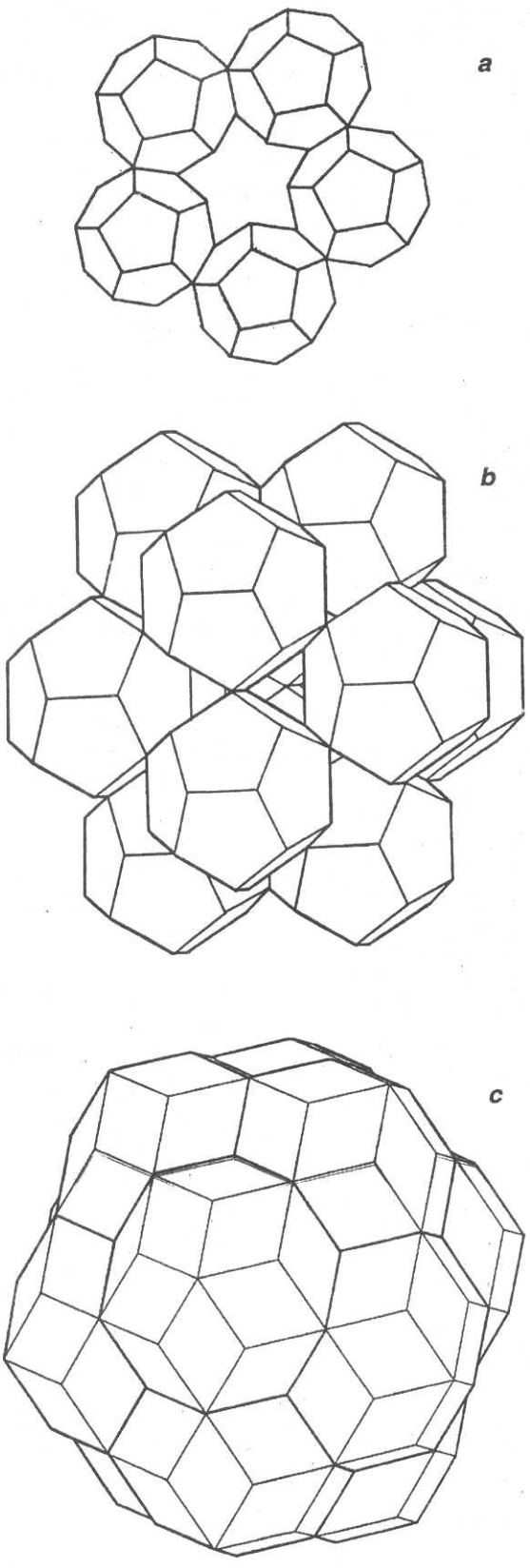

Figure 16. *a*, A ring of 5 edge-sharing pentagonal dodecahedra; *b*, a cluster of twelve. The interior of this figure is an icosidodecahedron ($3^2.5^2$).This configuration occurs in (*c*) the cluster of 12 triacontahedra that surround the centre of a τ^3 star polyhedron.

We now consider the pattern of overlapping clusters that arises when every triacontahedron of this covering is decorated with the 64 points indicated in Figure 8.

Clustering of triacontahedra

We now illustrate, by means of pictures, the various ways in which the triacontahedra enter into combinations in the covering pattern.

When the centres of the triacontahedra are placed at the golden mean positions in the way we have described, there are just four ways in which a pair of them can share vertices. The line of centres can be directed along a two-fold, a three-fold or a five-fold direction. In Table 1 the nature of the overlap is listed for each of the four kinds of bonds.

Other lengths occurring in the pattern are: Distance from centre of 30-hedron to mid-point of a face, τ^2; distance from centre of 30-hedron to a 3-fold vertex, $\tau\sqrt{3}$; distance from centre of 30-hedron to 5-fold vertex, $\tau\gamma$; short diagonal of an OU, $\tau^{-1}\sqrt{3}$; and long diagonal of a PU, $\tau^2\sqrt{3}$.

The four ways in which two triacontahedra can be joined will be referred to as 'type' 2′, 2, 3 or 5. Pairs of types 2, 3, and 5 are illustrated in Figures 12–14. The way

Table 1. Data for the four ways in which two of the triacontahedra can combine. $\gamma = \sqrt{(2+\tau)}$

Bond direction	Overlap region	Distance between centres	Number of shared external vertices
2'	Face	$2\tau^2$	4
2	Rhombic dodec.	2τ	6
3	Oblate unit	$\tau^2\sqrt{3}$	3
5	Rhombic icos.	γ	10

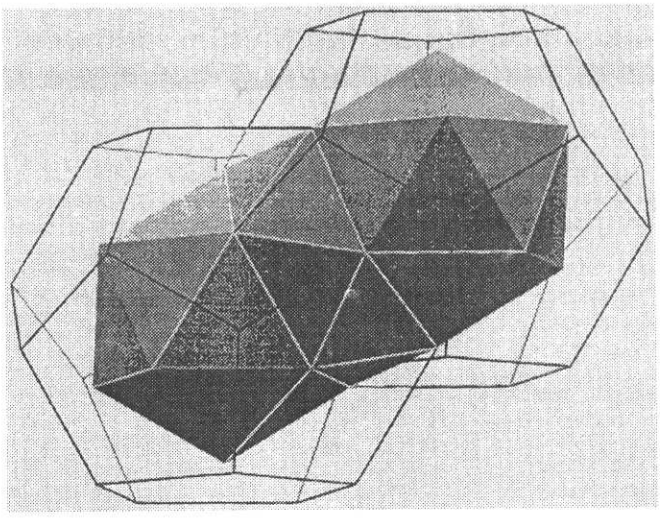

Figure 17. The configuration inside a type-5 pair. The two icosahedra are joined by a pentagonal antiprism which is not quite regular: the triangular faces are isosceles, with edges in the ratio $2 : \sqrt{3} \sim 1 \sim 0.86$.

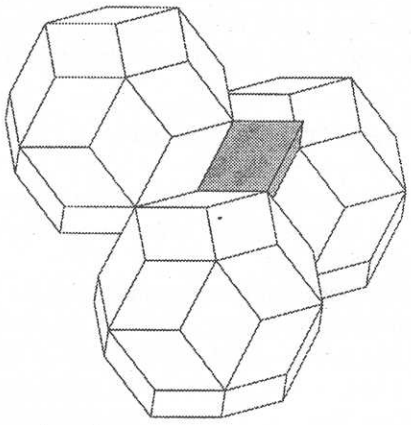

Figure 18. Three triacontahedra in face contact surrounding a PU. Three more, related by inversion, gives a configuration with $\bar{3}$ symmetry: six triacontahedra around the short diagonal of the τ^3 OU.

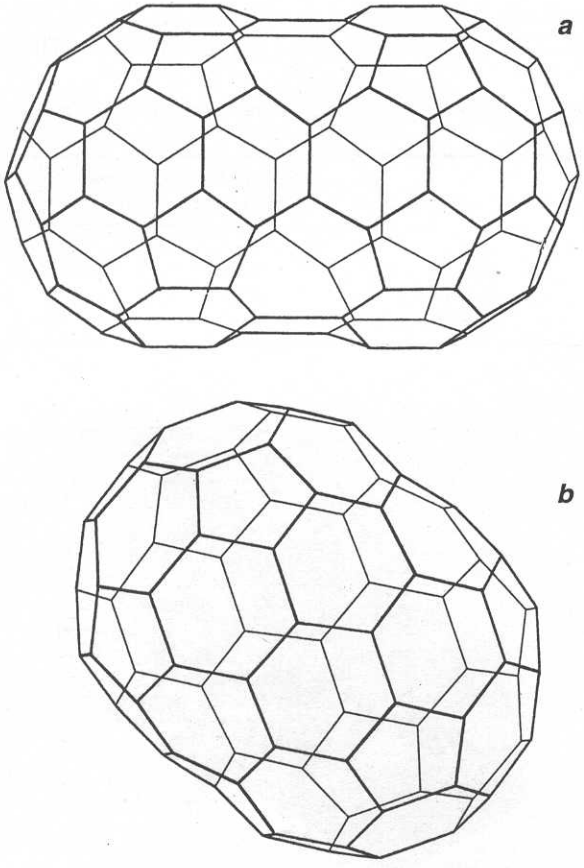

Figure 19. *a*, A 100-atom shell with 16 pentagons, 32 hexagons and 4 heptagons. Its symmetry is mmm; it occurs in the double cluster with type-2 bonding; *b*, An 80-atom shell with symmetry $\bar{5}$, occurring in the double cluster with type-5 bonding.

the four kinds of bonds between triacontahedron centres occur in the τ^3 units is shown in Figure 15.

If we consider the internal vertices of the triacontahedra of a pair, we find that in a type-2 pair the two inner dodecahedra share an edge. In a type-5 pair, the inner icosahedron/dodecahedron of each triacontahedron shares five vertices with the inner dodecahedron/icosahedron of the other. The various geometrical configurations that arise from these considerations are shown in Figures 16–18.

Application to clustering models of QC

The patterns produced by decorating the triacontrahedra with their 32 external and 32 internal vertices have arisen from purely geometrical considerations. A motivation for the study of these patterns is the light they may shed on the mode of growth of quasicrystals and their approximants, and the contribution they can make to the search for realistic clustering models of quasicrystal structure. Consider the 136-atom cluster that is a basic 'building block' in R-AlZnLi. Our 64-'atom' cluster can be converted to the 136-atom cluster by adding 12 atoms around the inner pentagonal dodecahedron, thus producing a 44-atom Bergman unit: this is then surrounded by a shell of 60 more atoms forming an Archimedean (5.6^2) between the inner and outer triacontahedra. The inner and the outer triacontahedra are in the ratio $1 : \tau$. The R phase is a bcc structure. The triacontahedral clusters are centred on the bcc positions, each is coordinated to 8 others by type-3 'bonding' and to six others by type-2′ 'bonding'. The arrangement of triacontahedra in the manner we have described suggests immediately a plausible model for the related quasicrystalline T2 phase. (Notice, incidentally, that when the dodecahedra of Figure 16 *b* are completed to triacontahedra by placing an atom over each pentagonal face, we obtain a cluster of twelve triacontahedra in face contact; the twelve innermost vertices form an icosahedron, and the innermost shells of the resulting cluster

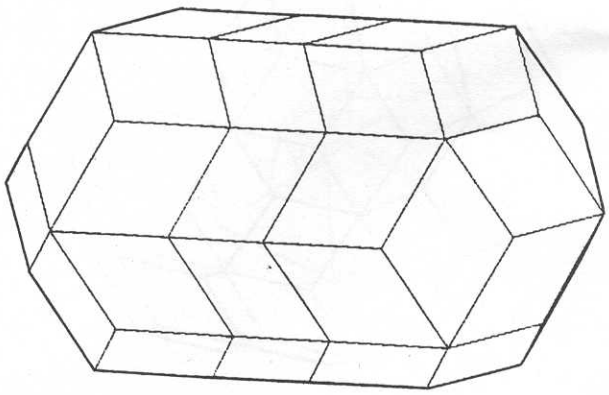

Figure 20. A rhombic 50-hedron. Two 'zones' have been inserted in a 30-hedron. In the type-5 pairing of the 'small' triacontahedra, the extra edges are reduced in length by a factor $\tau/2$.

form a 54 atom Mackay icosahedron! The occurrence of Bergman clusters and Mackay clusters in the same structure has been noted as a feature of other, quite different models[29].) The essential difference between the model proposed here and that of Audier and Guyot is that the centres of our triacontahedral clusters lie at the golden mean positions on the τ^3 edges, whereas Audier and Guyot placed them at the vertices of the τ^3 units.

When our basic 64-vertex clusters are completed to 136-atom clusters, the three types of double clusters (corresponding to the 'bonds' of types 2, 3, and 5 of Table 1) that are thereby produced have the following characteristics. In type-2 the two *inner* triacontahedra share a face and the two 60-atom shells can be 'merged' – the two inner triacontahedra can be surrounded by a shell with 16 pentagons, 34 hexagons and 4 heptagons ($V = 100$, $E = 150$, $F = 52$) (Figure 19 *a*). In type-3 the inner triacontahedron of each cluster shares a single vertex with the outer triacontahedron of the other. In type-5 the addition of atoms over the faces of the inner dodecahedra of Figure 17 produces the polyhedron shown in Figure 20 and the 60-atom shells are replaced by an elongated shell with 12 pentagons and 30 hexagons ($V = 80$, $E = 120$, $F = 42$) (Figure 19 *b*). In the complete structure arising from this model every cluster is, of course, coordinated with others that share atoms with it and completely surround it. To produce a realistically acceptable arrangement of atoms, some of the vertices need to remain unoccupied, and certain close pairs of vertices need to be replaced by a single atom at their mean position to produce an acceptable realistic arrangement of atoms. These small changes to the abstract geometrical pattern are minor and *systematic*. As in the model proposed by Audier and Guyot, in the complete pattern the 60-atom (5.6^2) shells of isolated clusters will 'merge' to produce more elaborate configurations with 5-, 6-, 7- and 8-membered rings. The atoms in this layer of the structure are perhaps best thought of as 'glue atoms' that fill in gaps in the growing structure, whose basic 'building-blocks' are large and small triacontahedra (in the ratio $1 : \tau$).

1. Shechtman, D., Blech, I., Gratias, D. and Cahn, J. W., *Phys. Rev. Lett.*, 1984, **53**, 1951.
2. Penrose, R., *Bull. Inst. Math. Appl.*, 1974, **10**, 266.
3. Grünbaum, B. and Shephard, G. C , *Tilings and Patterns*, W.H. Freeman, San Fransisco, ch. 10, 1987.
4. Katz, A. and Duneau, M., *J. Phys.*, 1986, **47**, 181.
5. Levine, D. and Steinhardt, P. J., *Phys. Rev.*, 1986, **B34**, 596.
6. Kramer, P. and Neri, R., *Acta Crystallogr.*, 1984, **A40**, 580.
7. Elser, V. and Henley, H. L., *Phys. Rev. Lett.*, 1985, **55**, 2883.
8. Guyot, P. and Audier, M., *Philos. Mag.*, 1985, **B52**, L15–L19.
9. Li, X. Z., *Acta Crystallogr. B*, 1995, **51**, 265–270.
10. Lord, E. A., *Curr. Sci.*, 1991, **61**, 313–319.
11. Mackay, A. L., *Acta Crystallogr.*, 1962, **15**, 916–918.
12. Bergman, G., Waugh, J. L. T. and Pauling, L., *Acta Crystallogr.*, 1957, **10**, 2454.
13. Audier, M. and Guyot, P., Proceedings of the I.L.L./CODEST Workshop (eds Janot, C. and Dubois, J. M.), 21–25 March, Grenoble, 1988, pp. 193–215.
14. Audier, M., Pannetier, J., LeBlanc, M., Janot., C., Lang, J. M. and Dubost, B., *Physica B*, 1988, **153**, 136.
15. Aslanov, L. A., *Acta Crystallogr.*, 1991, **A47**, 63.
16. Henley, H. L. and Elser, V., *Philos. Mag.*, 1986, **B56**, L59.
17. Romeau, D. and Aragon, J. L., *Crystal-Quasicrystal Transitions* (eds Yacaman, M. J. and Torres, M.), 1993, pp. 193–215.
18. Janot, C., *J. Phys. (Condensed Matter)*, 1997, **9**, 1493–1508.
19. Berger, R., *Mem. Am. Math. Soc.*, 1966, No. 66.
20. Penrose, R., *Eureka*, 1978, **39**, 16; reprinted in *Math. Intell.*, 1979, **2**, 32.
21. Gummelt, P., Proceedings of the 5th International Conference on Quasicrystals (eds Janot, C. and Mosseri, R.), 1995, pp. 84–87.
22. Gardner, M., *Sci. Am.*, 1977, 110.
23. Burkov, S. E., *J. Phys. I*, 1992, **2**, 695–706.
24. Jeong, H. C. and Steinhardt, P. J., *Phys. Rev. B*, 1997, **55**, 3520–3632.
25. Steinhardt, P. J., Jeong, H. C., Saitoh, K., Tanaka, M., Abe, E. and Tsai,. A. P., *Nature*, 1998, **396**, 55–57.
26. Sasisekharan, V., *Pramana*, 1986, **26**, 283–293.
27. Mackay, A. L., *J. Microsc.*, 1987, **146**, 233–243.
28. Mackay, A. L., *Sov. Phys. Crystallogr.*, 1981, **26**, 517–522.
29. Janot, C., Loreto, L., Farinato, R., Mancini, L., Baruchel, J. and Gastaldi, J., in Quasicrystals Symposium (eds Dubois, J.-M. *et al.*), 30 Nov.–2 Dec., Boston, Massachusetts, Materials Research Society, Warrendale, Pennsylvania, 1998, p. 55.

Received 4 August 1999; revised accepted 26 October 1999